Geol. Mag. **156** (*7*), *2019, pp. 1247–1264* © *Cambridge University Press 2018*
doi:10.1017/S0016756818000535

Reconstruction of the Cryogenian palaeogeography in the Yangtze Domain: constraints from detrital age patterns

YU LIU*‡, KUNGUANG YANG*‡†, ALI POLAT§¶ & XIAO MA*‡

*School of Earth Sciences, China University of Geosciences Wuhan, Wuhan 430074, China
‡Key Laboratory of Tectonics and Petroleum Resources, Ministry of Education, China University of Geosciences Wuhan, Wuhan 430074, China
§Department of Earth and Environmental Sciences, University of Windsor, Windsor, Ontario, N9B 3P4, Canada
¶Centre for Global Tectonics, School of Earth Sciences, China University of Geosciences Wuhan, Wuhan, 430074, China

(*Received* 16 February 2018; *accepted* 15 June 2018; *first published online* 20 August 2018)

Abstract – Detrital zircons are often used to constrain the maximum sedimentary age of strata and sedimentary provenance. This study aimed at reconstructing the Cryogenian palaeogeography of the Yangtze Domain based on U–Pb ages and Lu–Hf isotopic signatures of detrital zircons from sandstones in the southeastern part of the Yangtze Domain. U–Pb ages of the youngest detrital zircon grains from the Niuguping, Gucheng and Datangpo formations yielded average ages of 712 ± 24 Ma, 679.2 ± 6.2 Ma and 665.1 ± 7.4 Ma, respectively, which are close to the depositional ages of their respective formations. An integrated study of detrital zircon Lu–Hf isotopes and U–Pb ages from three samples revealed six main peak ages in the samples from the Anhua section at *c*. 680 Ma, *c*. 780 Ma, *c*. 820 Ma, *c*. 940 Ma, *c*. 2000 Ma and *c*. 2500 Ma. The characteristics of the U–Pb ages and Hf isotopes indicate a link between the north and southeast margins of the Yangtze Domain as early as *c*. 680 Ma, and the provenance of the coeval sedimentary sequences in the SE Yangtze Domain was the South Qinling Block on the northern margin of the Yangtze Domain. The provenance analysis on the *c*. 680 Ma detritus composing upper Neoproterozoic strata in the Yangtze Domain revealed that the detritus was transported southward from South Qinling to the southeast margin of the Yangtze Domain through the Exi Strait, but was hindered by the Jiangnan Orogenic Belt.

Keywords: South China, western Hunan, detrital zircons, provenance, U–Pb dating, Hf isotopes

1. Introduction

Clastic sediments are natural samples and ideal materials for studying the formation, evolution and chemical composition of the continental crust (Jahn, Gallet & Han, 2001; McLennan, 2001; Rudnick & Gao, 2003). The ideal aim of detrital zircon geochronology is to trace the transportation of clastic materials from their source area to the sedimentary basin. *In situ* U–Pb and Lu–Hf isotopic data from detrital zircons in clastic sediments and sedimentary rocks are used to identify provenance in sedimentary basins and reveal major magmatic events that occurred in the source region (Fedo, Sircombe & Rainbird, 2003; Andersen, 2005; Zhang *et al*. 2006*a*; Liu, X. M. *et al*. 2008; Belousova *et al*. 2012; Gehrels, 2012; Andersen, Kristoffersen & Elburg, 2016; Linol *et al*. 2016; Chen *et al*. 2016, 2018; Wang *et al*. 2017). Integrated analyses of detrital zircon U–Pb and Hf isotopes have thus become a powerful tool for deciphering provenance variation in a sedimentary basin during sedimentation and the denudation history of source regions (e.g. Myrow *et al*. 2010; Zhang *et al*. 2012; Wang, W. *et al*. 2013).

The assembly and break-up of Rodinia is an important geological event in geological history. The break-up of Rodinia (870–560 Ma) had a significant influence on the evolution history of South China (Li *et al*. 2008). Nevertheless, magmatic events recording the break-up of Rodinia in the Yangtze Domain (YGD) have been observed only up to 750 Ma (Xia *et al*. 2018 and references therein). Few tuff records from the Cryogenian period have been observed in the YGD. Although necessary reports about magmatic rocks are lacking (Zhao *et al*. 2011 and references therein; Dong & Santosh, 2016 and references therein), a large number of detrital zircons from this period have been recorded in the clastic rocks of the YGD (Yin *et al*. 2006; Liu, X. M *et al*. 2008; Zhang, Jiang & Han, 2008; Ling *et al*. 2010; Wang *et al*. 2010, 2012*a*,*b*; Wang, W. *et al*. 2013; Lan *et al*. 2015; Liu *et al*. 2015; Yu *et al*. 2016). Nevertheless, the source of the YGD sediments deposited during late Neoproterozoic time remains uncertain. Furthermore, the transportation of the upper Neoproterozoic detritus within the YGD has not been clearly constrained. Therefore, this study attempted to identify the source areas and migration processes and to reconstruct the Cryogenian palaeogeography of the YGD through detailed investigation of detrital zircons in the study area.

This study focused on U–Pb ages and Lu–Hf isotopic signatures of detrital zircons from sandstones in the southeastern part of the YGD deposited during the

†Author for correspondence: yangkunguang@163.com

Cryogenian period (Fig. 1). Our objective was to study the provenance and transport of the clastic material through zircon U–Pb–Lu–Hf isotopic analysis of the Nanhua strata, and to reconstruct the Cryogenian palaeogeography of the YGD.

2. Geological setting and sampling

2.a. Geological setting

The northern margin of the YGD is separated by the Mianlue–Bashan–Xiangguang Mesozoic overthrust fault (MBXF) from the South Qinling Block (SQB), which consists mainly of Middle to Upper Proterozoic volcano-sedimentary successions and Neoproterozoic intrusions overlain by sedimentary rocks (Dong *et al.* 2011). Precambrian basement rocks are exposed in the Yudongzi Group, Foping area, Douling Group, Wuguan Group, Yaolinghe Group and Wudangshan Group in the SQB (Zhang *et al.* 2001; Shi, Yu & Santosh, 2013). Of these, the Wudangshan Group is the most widely exposed basement strata in the SQB (Wang, R. R. *et al.* 2016) and its formation has been dated at 830–726 Ma using U–Pb ages of zircons from volcanic interlayers and sedimentary rocks (Ling *et al.* 2008, 2010; Wang, W. *et al.* 2013), although some studies reported an age of 783–675 Ma (Xia *et al.* 2008; Zhang *et al.* 2013), which is evidenced by the 632–688 Ma intruding plutons (Cai *et al.* 2007; Ling *et al.* 2008; Wang, W. *et al.* 2013; Zhu *et al.* 2015).

Several Neoproterozoic plutons occur in the SQB including the Fenghuangshan and Douling plutons. These plutons mainly comprise granitic and dioritic intrusions (Zhang *et al.* 2004; Yang *et al.* 2012; Dong & Santosh, 2016). They have been dated at *c.* 802–685 Ma, and show arc-related geochemical features (Zhang *et al.* 2004; Y. Y. Geng, unpub. M.Sc. thesis, China University of Geosciences, 2010; Liu *et al.* 2011; Li *et al.* 2012; Yang *et al.* 2012). In addition, the Xiaomoling Complex and some other small intrusions dated at *c.* 956–621 Ma also occur along the Shanyang fault (Niu *et al.* 2006; Liu *et al.* 2011, 2014; Wu, F. F. *et al.* 2012; Guo et *al.* 2014; Yan *et al.* 2014; Zhang *et al.* 2015; Hu, F. Y. *et al.* 2016; Wang, R. R. *et al.* 2016).

During the period of deposition of the Nanhua System, the YGD was composed of the Upper Yangtze Old Land (UYZOL), Ezhong Old Land (EZOL) and Jiangnan Old Land (JNOL) (Liu & Xu, 1994). The area on the southeast margin of the YGD is called the Nanhua rift basin, and the area on north margin of the YGD is called the South Qinling Sea Trough (Liu & Xu, 1994). The Nanhua rift basin on the southeast margin of the YGD was connected to the South Qinling Sea Trough through a channel called the Exi Strait (Fig. 2; Liu & Xu, 1994). The study area is located on the southeast margin of the YGD, where the western margin of the Jiangnan orogeny (JNO) lies (Fig. 1a, b). The main sedimentary formations of the Nanhua System include the Changan, Liangjiehe (Xieshuihe), Tiesiao (Gucheng), Datangpo and Nantuo formations. Two glaciation events probably occurred in the Changan and Gucheng formations in South China during the Sturtian glaciation (Lan *et al.* 2015). The Liangjiehe Formation belongs to an interglacial period, and the Nantuo Formation coincides with the Marinoan glaciation (Barfod *et al.* 2002; Chen *et al.* 2004). Chronological research has shown that the Marinoan glaciation ended at 635 Ma (Condon *et al.* 2005; Chu *et al.* 2005; Yin *et al.* 2005*a*,*b*; Zhang *et al.* 2005), and the Sturtian glaciation possibly ended at 670 Ma (Fanning & Link, 2004; Xiao *et al.* 2004; Yin *et al.* 2006; Yu *et al.* 2016). In the study area, the Nanhua System sedimentary strata are separated into the Gucheng, Datangpo and Nantuo formations, and it lacks the Changan formation. The Gucheng Formation has a direct unconformable contact with the Niuguping Formation at the top of the Banxi Group.

2.b. Sample collection

In our study, sedimentary rock samples were collected from a geological section located in Anhua, Dabu County, Hunan Province (Fig. 1b, c). These samples were used for geochronological (AH06, AH09 and AH14) and Hf isotopic analyses (AH06 and AH14). Furthermore, data on seven sections were obtained from previous studies. The lithology of the geological section is uniform, comprising mainly sandstone, tillite and sandy slate. AH09 is a slate sample from the top of the Niuguping Formation, AH06 is a tillite sample from the upper part of the Gucheng Formation (Fig. 1c) and AH14 is a sandstone sample from the middle part of the Datangpo Formation. Details on the regional stratigraphy and sampling lithology of the other sections are available in published literature (Fig. 2).

3. Analytical methods

Zircons were separated from crushed rock using a combination of conventional heavy liquid and magnetic separation techniques. Zircon grains were handpicked under a binocular microscope and cast in epoxy mounts together with zircon U–Pb standards 91500 and Plešovice, followed by polishing to section the crystals in half. All zircon grains were imaged in transmitted and reflected light as well as by cathodoluminescence (CL) to better reveal their internal structures.

The U–Pb isotopic compositions of the zircons were analysed at the State Key Laboratory of Geological Processes and Mineral Resources, China University of Geosciences, Wuhan. Laser sampling was performed using a GeoLas 2005 ArF excimer laser ablation system. An Agilent 7500a inductively coupled plasma mass spectrometry (ICP-MS) instrument was used to acquire ion-signal intensities. A 'wire' signal smoothing device is included in this laser ablation system, by which smooth signals are produced even at very low laser repetition rates down to 1 Hz (Hu *et al.* 2012*b*).

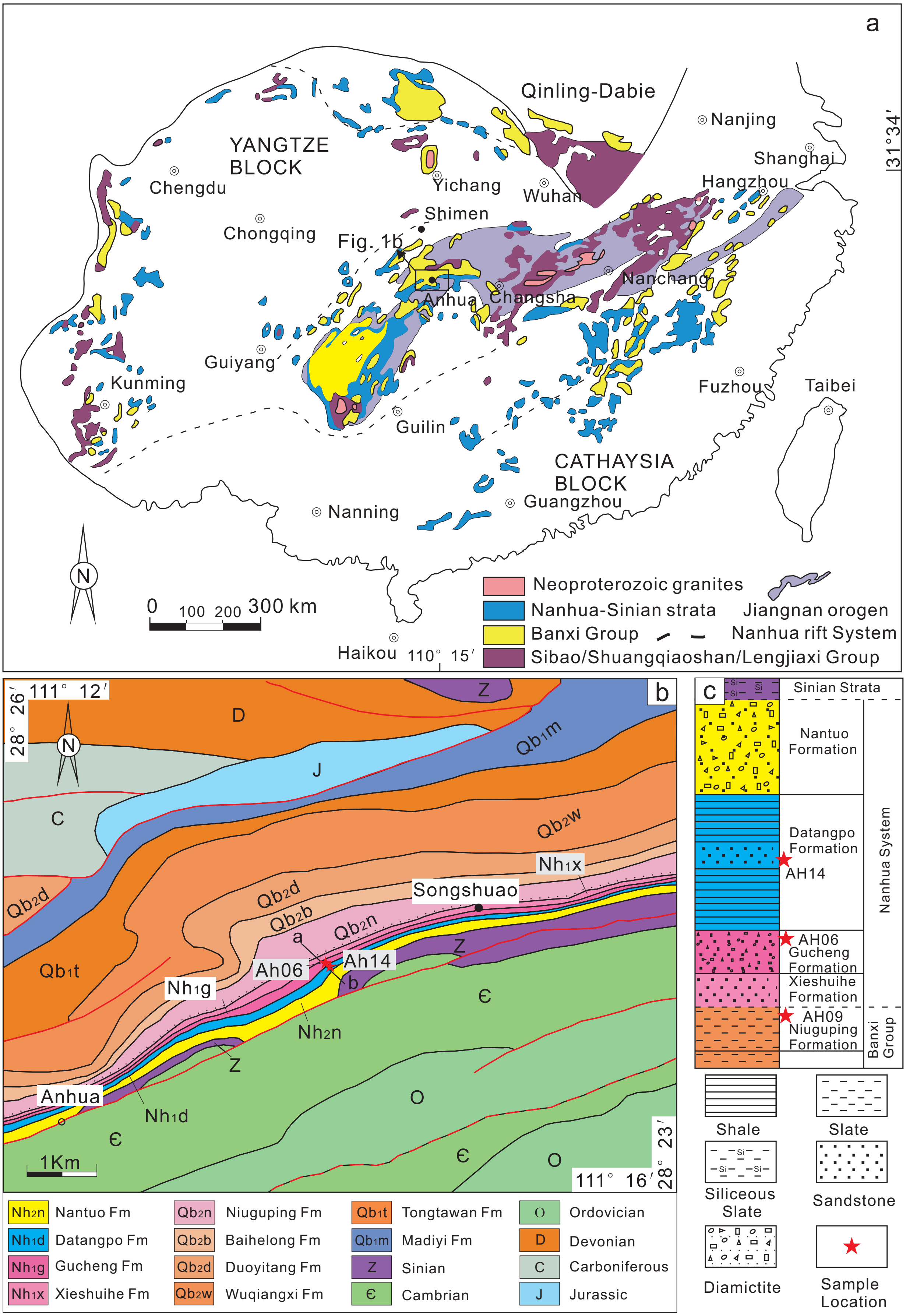

Figure 1. (Colour online) (a) Outcrops of Neoproterozoic igneous and sedimentary rocks and rift basins in the South China Block (modified from Du *et al*. 2013). (b) Simplified geological map of the study area showing the measured section. (c) Stratigraphic column in the Anhua area, with positions of sedimentary sampling marked.

https://doi.org/10.1017/S0016756818000535 Published online by Cambridge University Press

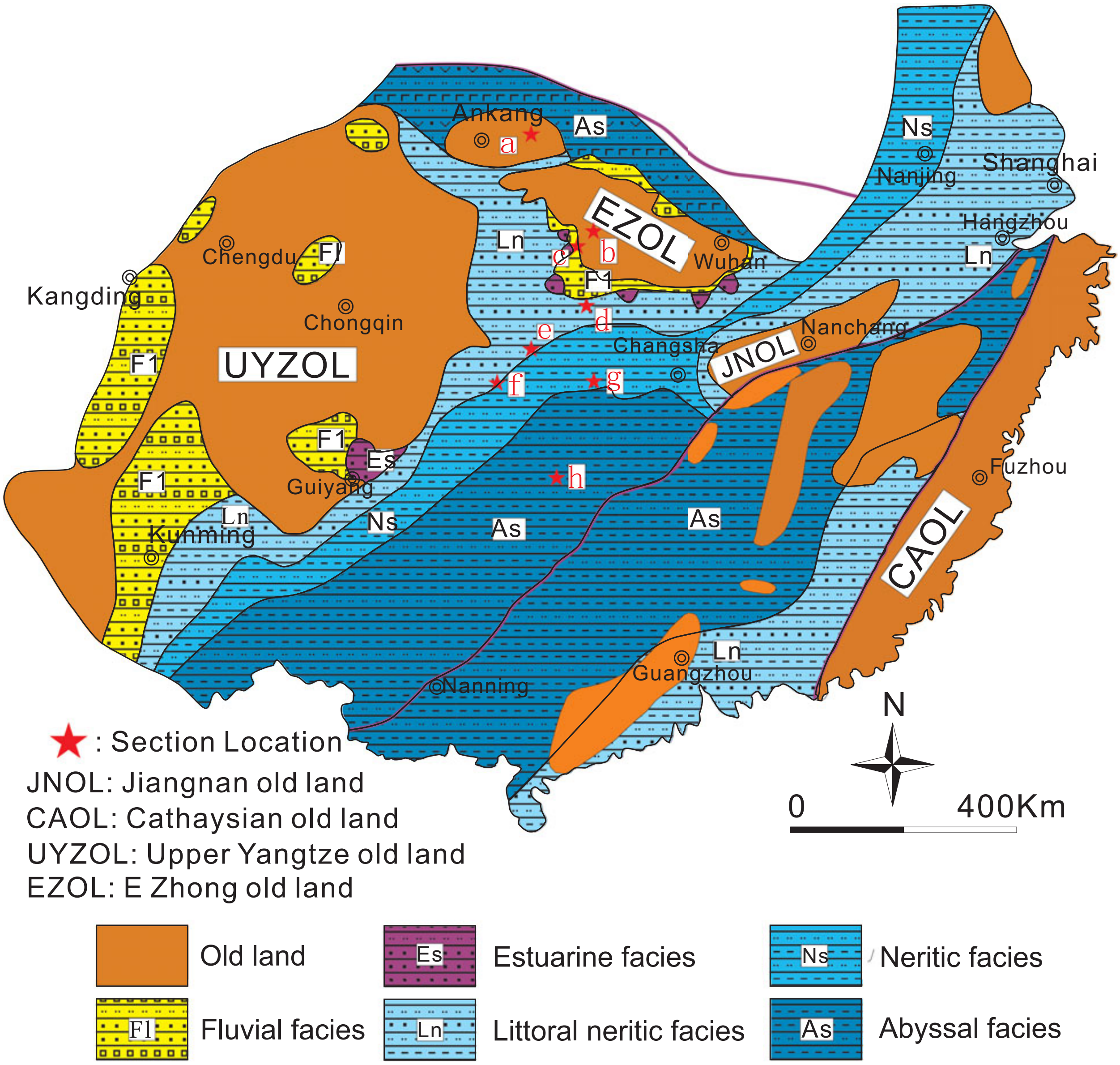

Figure 2. (Colour online) The 800–680 Ma palaeogeographic map of South China (revised after Liu & Xu, 1994; Wang & Li, 2003; Shu, 2006, 2012; Dong & Santosh, 2016).

Helium was used as the carrier gas to transport the ablated material from the laser ablation cell to the ICP-MS. The diameter of the laser ablation crater was 32 µm. Standard zircon 91500 was used as an external standard for U–Pb dating, and was analysed twice every five analyses. NIST610 glass was used as an external standard to normalize the U, Th and Pb concentrations of the unknowns. The detailed analytical procedures followed Liu *et al.* (2010*b*). Off-line selection and integration of background and analysis signals, and time-drift correction and quantitative calibration for U–Pb dating, were performed by ICPMSDataCal (Liu, Y. S. *et al*. 2008, 2010*a*). Calculation of concordia diagrams and weighted mean ages was done using Isoplot, with uncertainties quoted at the 1σ and 90 % confidence levels (Ludwig, 2003). The analytical data are presented in online Supplementary Material Table S1 available at http://journals.cambridge.org/geo.

The Lu–Hf isotope analysis was carried out *in situ* using a Neptune Plus multicollector-ICP-MS (Thermo Fisher Scientific, Germany) in combination with a Geolas 2005 excimer ArF laser ablation system (Lambda Physik, Göttingen, Germany) that was hosted at the State Key Laboratory of Biogeology and Environmental Geology, China University of Geosciences in Wuhan. All data were acquired on zircons in single spot ablation mode at a spot size of 44 µm in this study. Each measurement consisted of 20 s of acquisition of the background signal followed by 50 s of ablation signal acquisition. Detailed operating conditions for the laser ablation system and the MC-ICP-MS instrument and analytical method are the same as described by Hu *et al.* (2012*a*). The major limitation to accurate *in situ* zircon Hf isotope determination by laser ablation MC-ICP-MS is the very large isobaric interference from ^{176}Yb and, to a

https://doi.org/10.1017/S0016756818000535 Published online by Cambridge University Press

much lesser extent ^{176}Lu on ^{176}Hf (Woodhead *et al.* 2004). The ^{179}Hf/^{177}Hf and ^{173}Yb/^{171}Yb ratios were used to calculate the mass bias of Hf (βHf) and Yb (βYb), which were normalized to ^{179}Hf/^{177}Hf = 0.7325 and ^{173}Yb/^{171}Yb = 1.1248 (Blichert-Toft, Chauvel & Albarède, 1997) using an exponential correction for mass bias. Interference of ^{176}Yb on ^{176}Hf was corrected by measuring the interference-free ^{173}Yb isotope and using ^{176}Yb/^{173}Yb = 0.7876 (McCulloch, Rosman & De Laeter, 1977) to calculate ^{176}Yb/^{177}Hf. Similarly, the relatively minor interference of ^{176}Lu on ^{176}Hf was corrected by measuring the intensity of the interference-free ^{175}Lu isotope and using the recommended ^{176}Lu/^{175}Lu = 0.02656 (Blichert-Toft, Chauvel & Albarède, 1997) to calculate ^{176}Lu/^{177}Hf. Off-line selection and integration of analysis signals and mass bias calibrations were performed using ICPMSDataCal (Liu *et al.* 2010*a*). The analytical data are presented in online Supplementary Material Table S2 available at http://journals.cambridge.org/geo.

4. Results

4.a. CL images and Th/U ratios

Zircon grains from the three sedimentary rock samples collected in this study are light yellow to colourless and transparent to translucent. The grains exhibit a wide range of sizes and morphology. Representative CL images for the zircons from each sample are shown in Figure 3. The grains range in size from 50 to 200 µm, and mostly show a euhedral to subhedral morphology with clear oscillatory zoning. Most zircon grains from both the older and younger groups have Th/U ratios greater than 0.4, implying that a majority of them are of magmatic origin (Belousova *et al.* 2012). Two zircons (AH06-20, AH06-70) exhibited low Th/U ratios (< 0.1) (online Supplementary Material Table S1 available at http://journals.cambridge.org/geo) and one of them (AH06-20) showed a prominent metamorphic edge, indicating metamorphism (Fig. 3).

4.b. Zircon U–Pb geochronology

A total of 327 U–Pb analyses were acquired from the detrital zircon grains, and most analyses were located in the oscillatory core part of grains owing to the narrow width of the rim or mantle. Uncertainties on individual analyses in the data table and concordia plots are presented at 1σ. The U–Pb data are plotted in concordia diagrams in Figure 4 and the age histograms are also shown in Figure 4. In the following discussion, ^{206}Pb–^{238}U ages are used for zircon grains with ages less than 1000 Ma, whereas ^{207}Pb–^{206}Pb ages are used for zircons older than 1000 Ma, and the mean ages for pooled ^{206}Pb–^{238}U and ^{207}Pb–^{206}Pb results are quoted at the 90 % confidence level.

4.b.1. The Gucheng Formation (AH06)

Detrital zircon U–Pb ages were determined on 100 zircon grains from the tillite sample, AH06. All analyses on separated zircon grains are within 10 % of concordance and have Th/U ratios of 0.03–2.13, yielding ages ranging from 675 Ma to 2727 Ma (online Supplementary Material Table S1 available at http://journals.cambridge.org/geo). The Th/U ratios of AH06-20 and AH06-70 are 0.06 and 0.03, respectively. From the zircon isotope (Fig. 5, online Supplementary Material Table S3 available at http://journals.cambridge.org/geo) and CL image (Fig. 3) analyses, AH06-20 was determined to be a metamorphic zircon. Crystallization ages of the magmatic zircons are mainly grouped into two major age ranges: 675–687 Ma (n = 5) with an age peak at *c.* 683 Ma; and 721–899 Ma (n = 52) with two age peaks of *c.* 776 Ma and *c.* 816 Ma. These groups account for *c.* 5 % and 52 % of the total analyses. Two subordinate groups were observed in older age populations belonging to the Palaeoproterozoic (1939–2118 Ma, n = 24) and late Neoarchaean to early Palaeoproterozoic (2381–2619 Ma, n = 7) periods, with age peaks at *c.* 2033 Ma and *c.* 2497 Ma, respectively (Fig. 4). In addition, three Archaean zircons were identified in the sample with an age of *c.* 2727 Ma. The youngest group was defined using the weighted average age of 679.2 ± 6.2 Ma (MSWD = 0.52, n = 5), which served to constrain the maximum depositional age for the upper part of the Gucheng Formation in the Anhua region.

4.b.2. The Datangpo Formation (AH14)

A total of 111 analyses were conducted on the magmatic zones of zircon grains from the Datangpo sandstone (AH14). These zircons are mainly light yellow to colourless and translucent with Th/U ratios of 0.11–2.02. All of the analyses are concordant, yielding ages from 662 Ma to 2918 Ma. Age spectra can be classified into six groups: 662–685 Ma (n = 8), 701–799 Ma (n = 27), 805–879 Ma (n = 39), 923–944 Ma (n = 7), 1936– 2099 Ma (n = 15) and 2205–2637 Ma (n = 12), with six main age peaks at *c.* 663 Ma, *c.* 769 Ma, *c.* 847 Ma, *c.* 938 Ma, *c.* 2018 Ma and *c.* 2491 Ma, respectively (online Supplementary Material Table S1 available at http://journals.cambridge.org/geo). The corresponding proportions of these six main age clusters to the total analyses are 7.2 %, 24.3 %, 35.2 %, 6.3 %, 13.5 % and 10.8 %. In addition, three Archaean zircons of *c.* 2887 Ma, 2889 Ma and 2918 Ma could be identified in the sample (Fig. 4). Considering the weighted average age, the youngest group has a ^{206}Pb–^{238}U age of 665.1 ± 7.4 Ma (MSWD = 0.082, n = 6), which implies an upper age limit for the deposition of the bottom of the Datangpo Formation.

4.b.3. The Niuguping Formation (AH09)

Detrital zircon U–Pb ages were determined for 116 zircon grains from sample AH09. All analyses on separated zircon grains are within 10 % of concordance and have Th/U ratios of 0.29–2.22, yielding ages ranging

https://doi.org/10.1017/S0016756818000535 Published online by Cambridge University Press

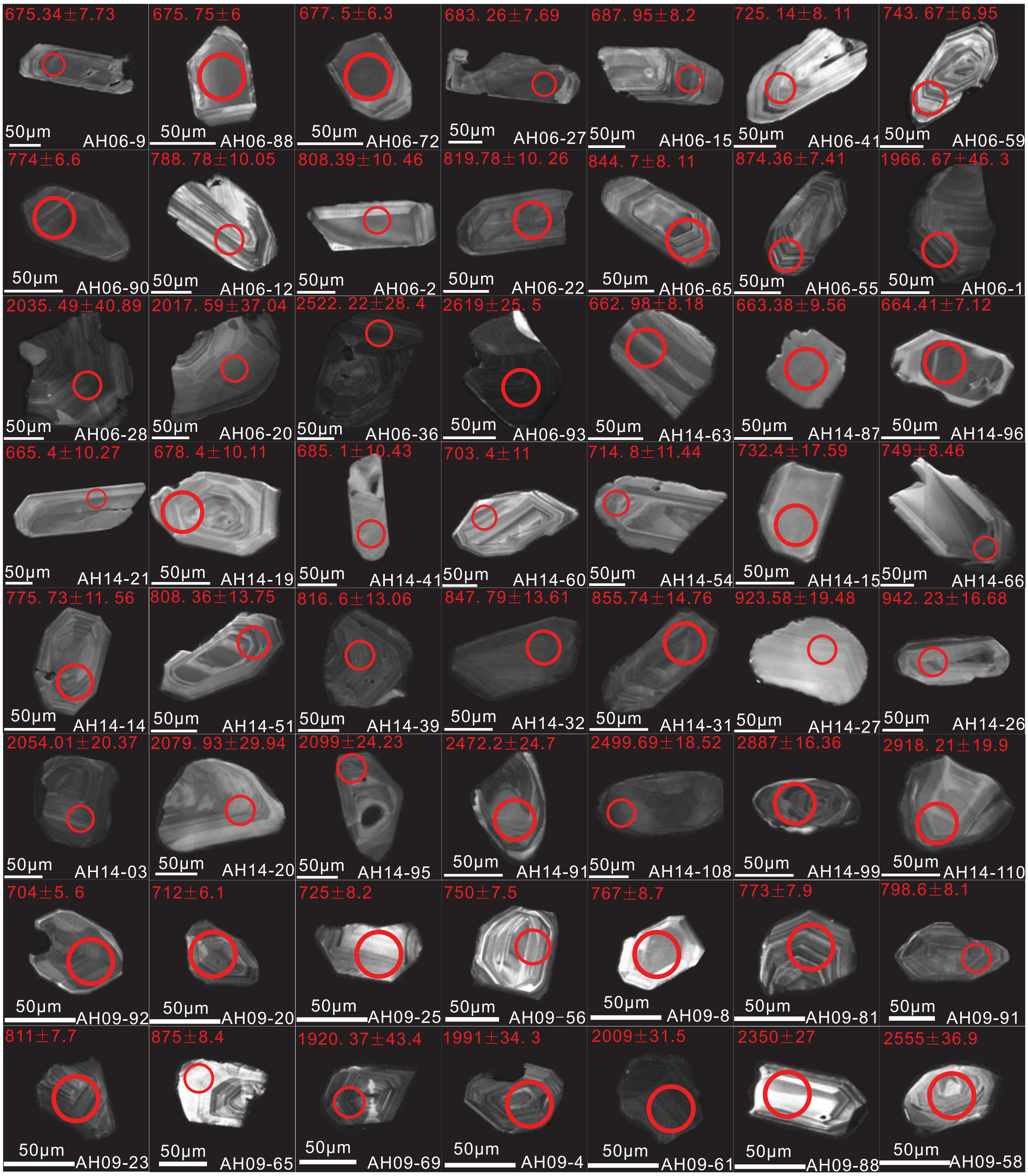

Figure 3. (Colour online) Typical cathodoluminescence (CL) images of zircon grains from samples AH06, AH14 and AH09. The circles show LA-ICP-MS dating spots. The zircon U–Pb ages with 1 σ uncertainties are listed next to the circles.

from 704 Ma to 3318 Ma (online Supplementary Material Table S1 available at http://journals.cambridge.org/geo). Crystallization ages of the magmatic zircons are mainly grouped into two major age ranges: 704–725 Ma (n = 3) with an age peak at *c*. 712 Ma; and 731–925 Ma (n = 78) with two age peaks of *c*. 770 Ma and *c*. 871 Ma, accounting for *c*. 3 % and 67 % of the total analyses. Two subordinate groups are in older age populations of the Palaeoproterozoic (1816–2076 Ma, n = 19) and late Neoarchaean to early Palaeoproterozoic (2345–2655 Ma, n = 13) (Fig. 4). In addition, two Mesoproterozoic zircons with ages of *c*. 1342 Ma and *c*. 1387 Ma were identified in the sample along with one Archaean zircon (*c*. 3318 Ma). From the weighted average age, the youngest group was defined to be 712 ± 24 Ma (MSWD = 2.3, n = 3), constraining the maximum depositional age for the upper part of the Niuguping Formation in the Anhua region.

https://doi.org/10.1017/S0016756818000535 Published online by Cambridge University Press

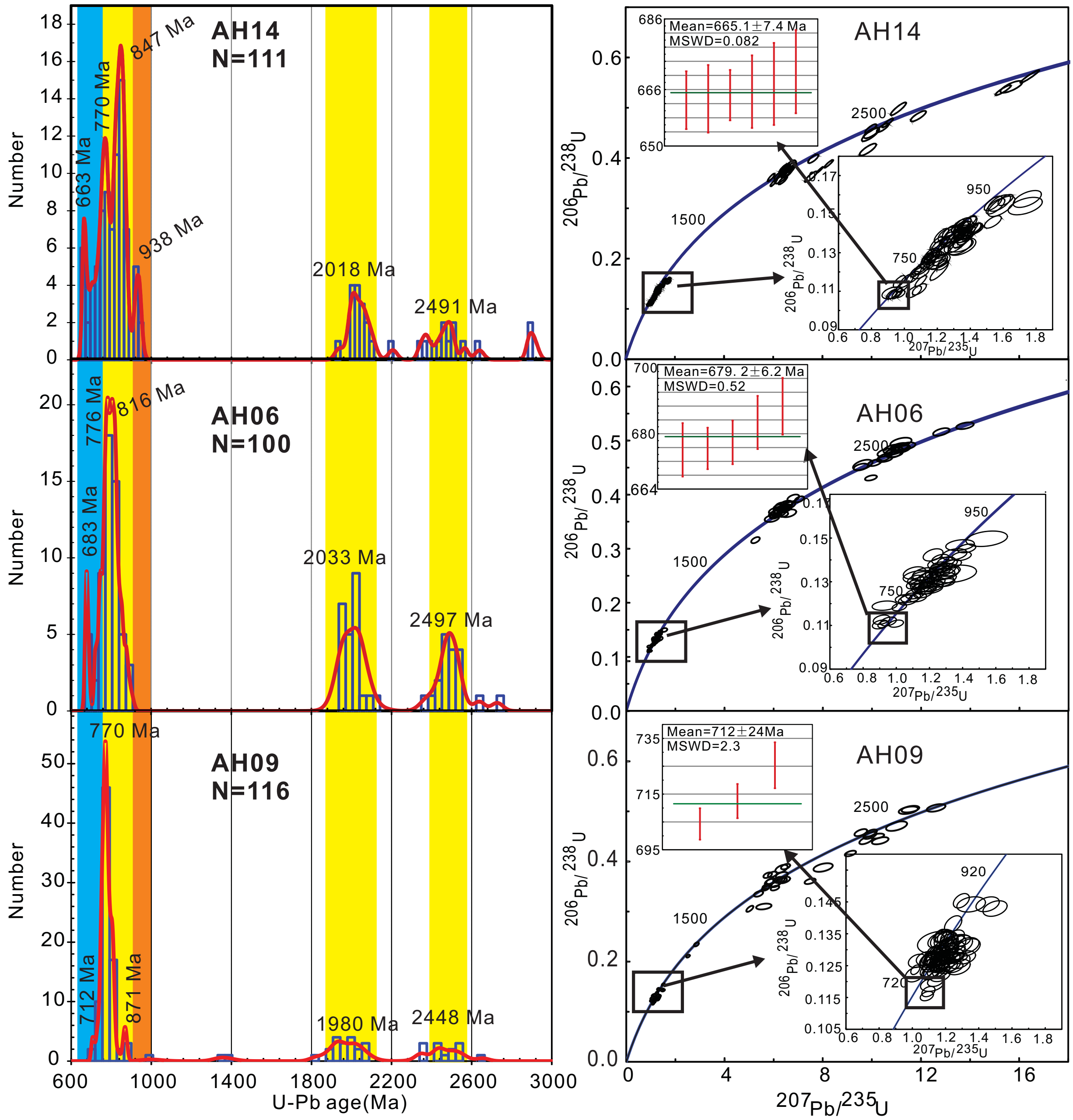

Figure 4. (Colour online) Diagrams of U–Pb ages, concordia plots of zircons and weighted mean ages from the samples in Anhua, Hunan.

4.c. *In situ* Hf isotope composition

A total of 85 zircon grains showing concordant U–Pb ages were selected for *in situ* Hf isotopic analyses from two sedimentary rocks. The results are given in online Supplementary Material Table S2 (available at http://journals.cambridge.org/geo).

AH06 showed age patterns similar to those of the four main U–Pb age groups of 675–687 Ma, 721–899 Ma, 1939–2118 Ma and 2381–2619 Ma. Neoproterozoic grains have variable $\varepsilon_{Hf}(t)$ values (−41.4 to 16.6) and T_{DM2} ages (727–3807 Ma), indicating mixing between a Neoproterozoic juvenile component and crustal material. In addition, the youngest group of Neoproterozoic grains have variable $\varepsilon_{Hf}(t)$ values (−0.36 to 2.61) and T_{DM2} ages (1349–1053 Ma), but only one zircon $\varepsilon_{Hf}(t)$ value was negative. Palaeoproterozoic zircon grains also showed a wide range of $\varepsilon_{Hf}(t)$ values from −24.5 to 12.1 and Hf model ages (T_{DM2}) from 1850 Ma to 3859 Ma, and all of them showed negative $\varepsilon_{Hf}(t)$ values, except for one. The late Archaean zircon grains have variable $\varepsilon_{Hf}(t)$ values (−11.98 to 3.12) and T_{DM2} ages (2771–3563 Ma). In addition, one zircon (2727 Ma) displayed an $\varepsilon_{Hf}(t)$ value of −2.5 and T_{DM2} of 3253 Ma.

AH14 also showed a similar age pattern with the five main U–Pb age groups of 662–685 Ma, 701–799 Ma, 805–879 Ma, 923–944 Ma, 1936–2099 Ma and 2205–2637 Ma. Neoproterozoic grains have variable $\varepsilon_{Hf}(t)$ values (−16.2 to 13.55) and T_{DM2} ages

https://doi.org/10.1017/S0016756818000535 Published online by Cambridge University Press

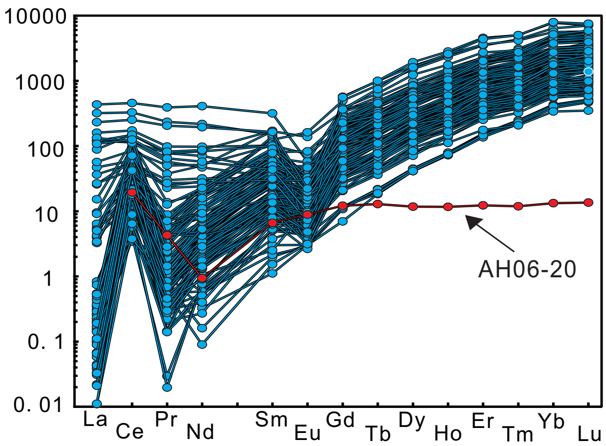

Figure 5. (Colour online) Chondrite-normalized rare earth element patterns of zircons in sample AH06 (online Supplementary Material Table S3 available at http://journals.cambridge.org/geo).

(933–2481 Ma), indicating mixing between a Neoproterozoic juvenile component and crustal material. The youngest group of Neoproterozoic grains have variable ε_{Hf}(t) values (−1.32 to 7.02) and T_{DM2} ages (933–1546 Ma), but only one zircon ε_{Hf}(t) value is negative. Palaeoproterozoic zircon grains also showed a wide range of ε_{Hf} (t) values from −11.6 to −4.1 and Hf model ages (T_{DM2}) from 2805 Ma to 3527 Ma; all of them showed negative ε_{Hf}(t) values, except for one. The two Archaean zircon grains have ε_{Hf}(t) values of −1.2 and −3.9, as well as T_{DM2} ages of 3113 Ma and 3451 Ma.

5. Discussion

5.a. Provenance analysis of samples

This study analysed one sample from the Banxi Group and two others from the Nanhua strata. As shown in Figure 4, the detrital zircon age patterns of the sedimentary rocks straddling the unconformity between the Banxi Group and the Nanhua strata are similar to each other. Both of the age spectra have two older age peaks (*c*. 2.0 Ga and *c*. 2.5 Ga), and two younger age peaks (*c*. 780 Ma and *c*. 820 Ma). However, the younger strata has one additional age peak (*c*. 680 Ma) compared to the older one. The southeastern margin of the YGD has no record of 680 Ma magmatic events, indicating that it is not the original source.

The distribution of detrital zircons in samples from different sedimentary rocks can provide clues for provenance characteristics (Rainbird, Hamilton & Young, 2001; Fonneland *et al*. 2004). The provenance characteristics could be analysed using the detrital zircon age spectra for the two middle–upper Nanhua System sedimentary samples from western Hunan.

Six main peak ages were obtained from three sedimentary samples in Anhua, Hunan: *c*. 680 Ma, *c*. 780 Ma, *c*. 820 Ma, *c*. 940 Ma, *c*. 2000 Ma and *c*. 2500 Ma. Furthermore, some magmatic zircon ages of *c*. 2900 Ma and *c*. 3300 Ma were obtained. During Neoproterozoic time, the southeastern YGD experienced two evolutionary stages, including a 1.0–0.82 Ga period of subduction collision and a 800–635 Ma period of stretching tension (Charvet, 2013 and references therein). Unlike the southeast, the north YGD experienced a long-term accretionary orogeny caused by the 1.0–0.7 Ga continuous collision and accretion (Dong & Santosh, 2016 and references therein). In contrast to the different magmatic evolution histories in the north and southeast margin of the YGD, recent studies have revealed similar zircon age spectra for upper Neoproterozoic sequences from these two areas (Ling *et al*. 2010; Wang, W. *et al*. 2013; Dong & Santosh, 2016; Yang *et al*. 2018; Xia *et al*. 2018).

At present, few studies on the *c*. 680 Ma magmatic events in South China have been carried out. Source rocks of *c*. 680 Ma are represented by Neoproterozoic igneous rocks mainly in South Qinling on the northern margin of the YGD; this magmatic event may be related to the break-up of Rodinia (Fig. 6; Niu *et al*. 2006; Ling *et al*. 2008; Zhang *et al*. 2013; Hu, F. Y. *et al*. 2016). Neoproterozoic magmatic rocks and detrital zircons, especially of 860–720 Ma age, are extensively distributed around the YGD (Zhang & Zheng, 2013). The two large-scale magmatic events of the Neoproterozoic (*c*. 750 Ma and *c*. 820 Ma) recorded the evolution of the Earth's crust during Neoproterozoic time, which is an important characteristic of South China (Wang *et al*. 2006; Zhang *et al*. 2006*a*; Zheng & Zhang, 2007). These activities may be related to the splitting of the Rodinia supercontinent. The peak detrital zircon ages obtained in this study (*c*. 776 Ma and *c*. 820 Ma; Fig. 4) confirm that the source of the study area rocks was the YGD and its provenance was related to the evolution of the Rodinia supercontinent during middle–late Neoproterozoic time. At present, a few igneous rocks of *c*. 924 Ma age exist in the YGD. Nevertheless, the Yanbian and Bikou groups (Fig. 6c), located in the western margin of the YGD and South Qinling, respectively, have a prominent age peak at *c*. 920 Ma. In this study, the Datangpo Formation (AH14) was found to have a zircon age peak of *c*. 938 Ma, which does not appear in the Gucheng Formation (AH06) (Fig. 4), indicating the likelihood of an event that led to the addition of material from new sources. Magmatic activities of Palaeoproterozoic age (*c*. 2.0 Ga) are distributed in the northern areas of the YGD, such as the areas of Kongling, Jinshan, Liantuo and South Qinling (Zhang *et al*. 2006*c*; Sun *et al*. 2008; Wu, Y. B. *et al*. 2012; Yin *et al*. 2013; Nie *et al*. 2016; Wang, W. *et al*. 2016), which records the tectonic heating events of the Kongling Complex and the crustal reconstruction event in the north of the YGD (Zheng & Zhang, 2007 and references therein). Archaean zircons (*c*. 2500 Ma) are from the Yichang Kongling trondhjemitic gneiss and migmatite (Wu *et al*. 2014), and the Hu Yang Po Group and intrusion of potassium granite in Zhongxiang (Wang, L. J. *et al*. 2013). Furthermore, a current study reported large

https://doi.org/10.1017/S0016756818000535 Published online by Cambridge University Press

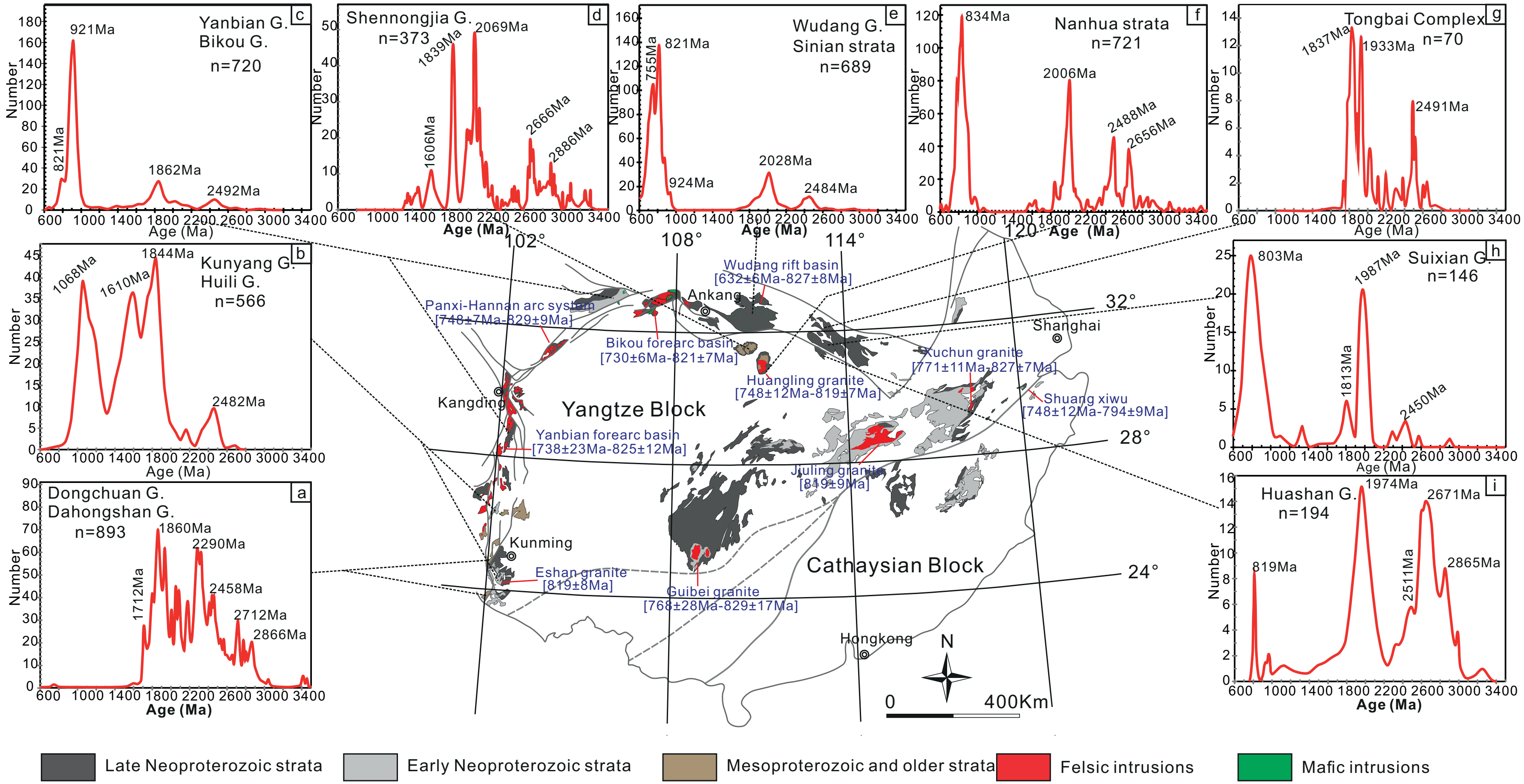

Figure 6. (Colour online) Comparison of probabilistic histograms of age distributions for the detrital zircons from Precambrian (meta)sedimentary rocks and the distribution of Neoproterozoic igneous rocks in various parts of the Yangtze Domain (data from Zhao *et al.* 2011 and references therein; Yang *et al.* 2018 and references therein; samples in this study; modified from Yang *et al.* 2018). Geologic map of South China modified after the 1:2 500 000 geologic map of CAGS (2004). (Dongchuan Gp: 1.8–1.4 Ga; Dahongshan Gp: 1.8–1.4 Ga; Kunyang Gp: 1.2–1.0 Ga; Huili Gp: 1.2–1.0 Ga; Yanbian Gp: 825–738 Ma; Bikou Gp: 821–730 Ma; Shennongjia Gp: 1.4–1.0 Ga; Wudang Gp: *c.* 780 Ma; Nanhua System: 720–635 Ma; Suixian Gp: *c.* 760 Ma; Huashan Gp: *c.* 820 Ma.)

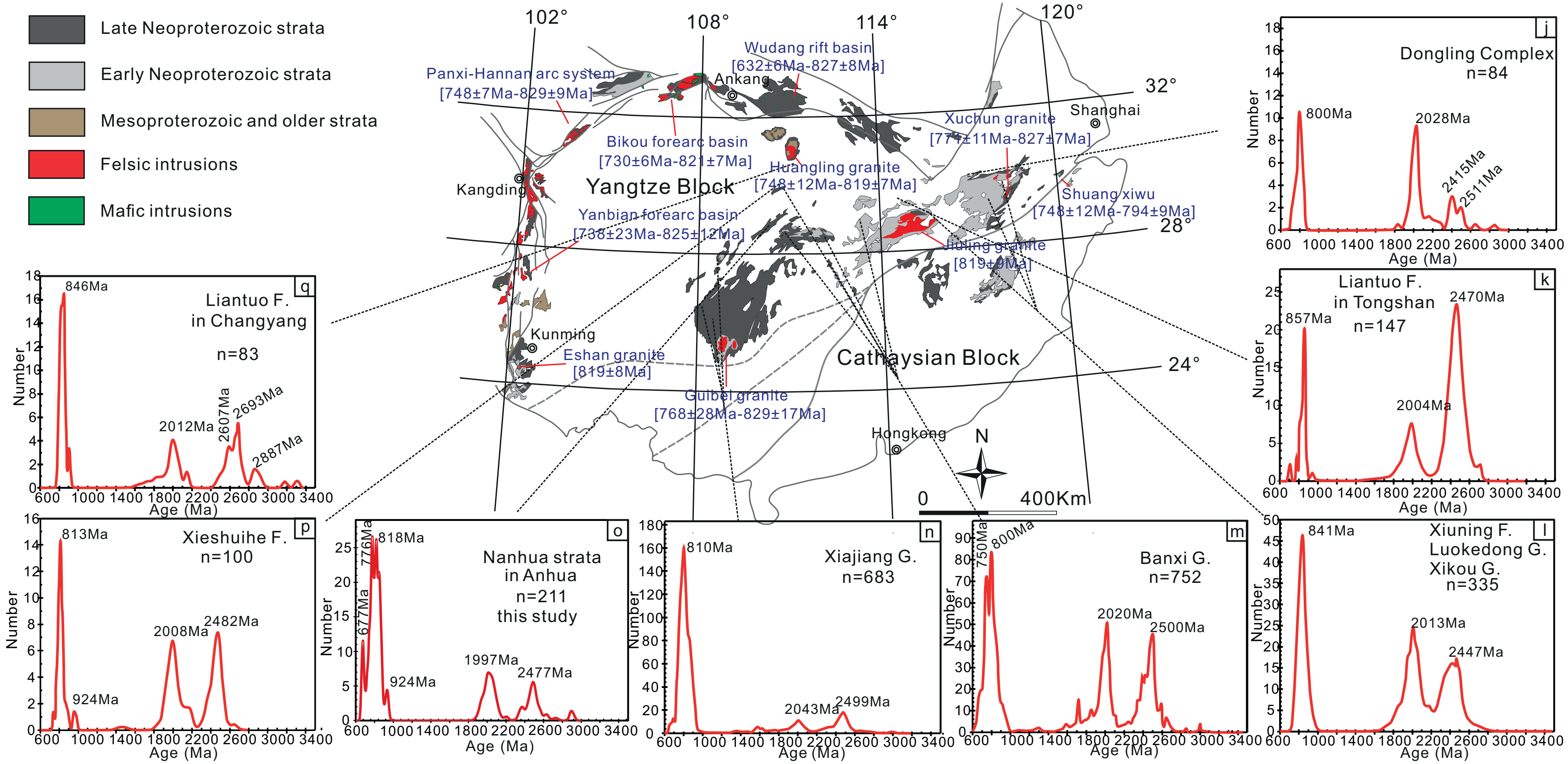

Figure 6. (Continued) (Colour online). Comparison of probabilistic histograms of age distributions for the detrital zircons from Precambrian (meta)sedimentary rocks and the distribution of Neoproterozoic igneous rocks in various parts of the Yangtze Domain. (Liantuo Fm: *c*.780 Ma; Xiuning Fm: *c*. 730 Ma; Luokedong Fm: *c*. 767 Ma; Xikou Gp: 780–720 Ma; Banxi Gp: 820–720 Ma; Xiajiang Gp: 820–720 Ma; Xieshuihe Fm: *c*. 690 Ma).

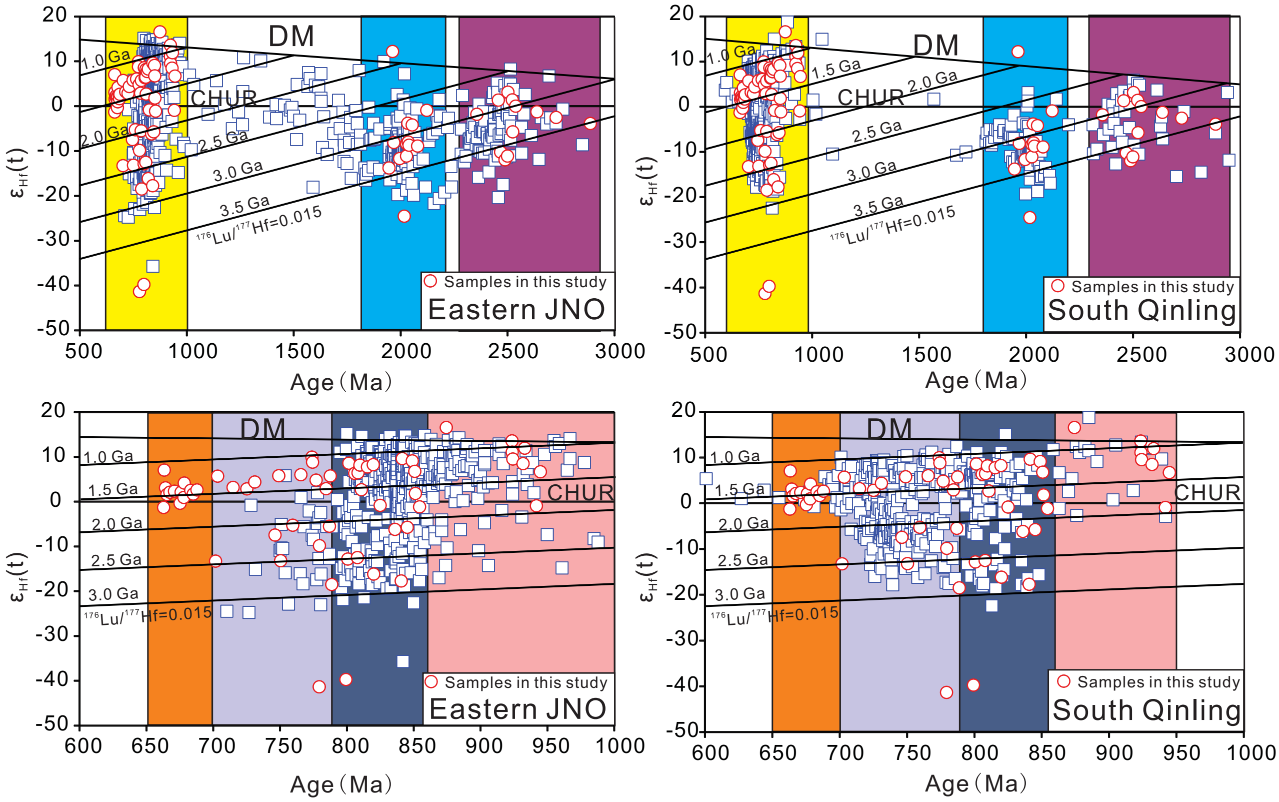

Figure 7. (Colour online) Plots of $\varepsilon_{Hf}(t)$ values versus crystallization ages of zircons from South Qinling and the eastern JNO (data from Yang *et al.* 2018 and references therein; samples in this study). DM – depleted mantle; CHUR – chondritic uniform reservoir.

magmatic rocks of *c.* 2.5 Ga as observed in the Douling Group, South Qinling (Hu *et al.* 2013; Wu *et al.* 2014). The 2.5 Ga age peak is characteristic of the YGD (Wu *et al.* 2002; Li, Li & He, 2012). Although Archaean magmatic activity has rarely been reported in the YGD at present, magmatic activity should have taken place during this period, as it is an important period of crustal growth in South China. Among the samples, the ages of the oldest populations range from 2.4 Ga to 2.6 Ga, reflecting the magmatic event. Zircons aged *c.* 2.9 Ga are widespread within the YGD, such as in TTG gneiss and other rocks of the Kongling Complex in the north of the YGD (Qiu *et al.* 2000; Zhang *et al.* 2006*b*). The existence of a small amount of zircon of *c.* 2.9 Ga in the study area indicates that the southeastern margin of the YGD received small quantities of input from the north YGD.

In this study, a total of 6767 U–Pb ages for detrital zircons from Precambrian metasedimentary strata around the YGD were collected for comparison (Fig. 6a–q). All detrital zircons exhibited the age peak characteristics of the Precambrian basement in the YGD (Fig. 6). The Nanhua strata in the study area appears to have the features of a mix of former sequences with age peaks at *c.* 0.68 Ga, *c.* 0.8 Ga, *c.* 0.9 Ga, *c.* 2.0 Ga and *c.* 2.5 Ga (Fig. 6o). Compared with the detrital zircon age data in the Precambrian basement in the periphery of the YGD, the Wudang Group, Xiuning Formation, Banxi Group and Xiajing Group developed along the Exi Strait show the same age peak characteristics with age peaks at *c.* 0.8 Ga, *c.* 2.0 Ga and *c.* 2.5 Ga (Fig. 6e, j, l–n, p). A prominent *c.* 1.8 Ga age peak (Fig. 6a–c) was observed in the western and northwestern YGD, and a prominent age peak of *c.* 2.6 Ga was obtained in the Huangling granite, which are not found in the study area (Fig. 6f, q). It is unlikely that these two regions are sources of the study area. At present, the source composition of the study area is consistent with the eastern JNO and South Qinling, although there is a lack of *c.* 680 Ma sources in the eastern JNO (Fig. 6).

We determined the zircon $\varepsilon_{Hf}(t)$ values of South Qinling and the eastern JNO to distinguish the differences between the two regions. As shown in Figure 7, the two regions exhibited distinct $\varepsilon_{Hf}(t)$ value characteristics. In South Qinling (Fig. 7), a significant change occurred at *c.* 850 Ma, as marked by an increase in negative $\varepsilon_{Hf}(t)$ values of the <850 Ma detrital zircons relative to those at 950–850 Ma. Another change occurred at *c.* 700 Ma, as characterized by a reduction in negative $\varepsilon_{Hf}(t)$ values of the <700 Ma detrital zircons relative to those at 850–700 Ma. Furthermore, the negative and positive values were relatively uniform for the age range of 850–700 Ma. In the eastern JNO (Fig. 7), zircons show mostly positive $\varepsilon_{Hf}(t)$ values at >870 Ma, both negative and positive $\varepsilon_{Hf}(t)$ values at 870–810 Ma, and dominantly negative $\varepsilon_{Hf}(t)$ values at <810 Ma. In this study, the $\varepsilon_{Hf}(t)$ values of 13 detrital zircons from our samples of *c.* 680 Ma age are generally positive except for two magmatic zircons,

https://doi.org/10.1017/S0016756818000535 Published online by Cambridge University Press

and the characteristics are generally in line with the characteristics of *c*. 680 Ma age zircons in South Qinling; however, this source is lacking in the eastern JNO (Fig. 7). Another difference is that zircons show mostly negative $\varepsilon_{Hf}(t)$ values at 850–700 Ma in the eastern JNO and show both negative and positive $\varepsilon_{Hf}(t)$ values at 850–700 Ma in South Qinling. The characteristics of the values at 850–700 Ma are the same as those of South Qinling (Fig. 7). In addition, the characteristics of the values at >850 Ma in our samples show similarities to those of South Qinling.

A metamorphic zircon (AH06-20) aged 2017.59 ± 37 Ma was also found (Figs 3, 5). Current research suggests that the main source of metamorphic zircons of *c*. 2.0 Ga age is the Kongling Complex (Zhang *et al*. 2006*c*; Wu *et al*. 2009; Yin *et al*. 2013), and metamorphic zircons of the same period are also found in the Douling Group of South Qinling (Nie *et al*. 2016). As mentioned above, the source of the study area is more likely to be the South Qinling than the Kongling area.

In summary, the provenance characteristics of the end of the Sturtian ice age (*c*. 660 Ma) in western Hunan are reflected in the crust formed by episodic accretion, which is related to supercontinent growth and cracking in the Archaean, Palaeoproterozoic and Neoproterozoic. We believe that at the end of the Sturtian ice age as early as *c*. 680 Ma, South Qinling was the main source area for western Hunan.

5.b. Migration process of sedimentary provenance

As mentioned earlier, source rocks of *c*. 680 Ma are represented by Neoproterozoic igneous rocks mainly in the South Qinling area on the northern rim of the YGD, and the source of the study area rocks is South Qinling. The characteristic age peak of *c*. 680 Ma can be used to determine the transport of source materials from South Qinling to western Hunan.

In addition to the geological section investigated in this study, details of the regional stratigraphy and sampling lithology for the following other sections are available in the published literature: Wudang section, Yichang section, Changyang section, Shimen section, Guzhang section, Songtao section and Guibei section (Figs 8, 9).

Considering that the source of the study area rocks is South Qinling and not the EZOL, source materials may have been transported along the Exi Strait to the study area. A total of 2640 U–Pb ages for detrital zircons from eight sections along the Exi Strait were compiled (Figs 8, 9). As show in Figure 8, the main peaks of each profile are at *c*. 0.8 Ga, *c*. 2.0 Ga and *c*. 2.5 Ga, except for the Guzhang and Songtao sections (Fig. 8e, f: only counting tuff age). The Yichang and Changyang sections have an age peak of *c*. 2.6 Ga, which differs from the others, indicating that the source material from the Kongling area was transported to the Changyang area and was blocked from reaching western Hunan (Fig. 8b, c). Furthermore, the *c*. 680 Ma source material appeared to reach the Changyang area but not the Yichang area, which implies that the source material carrying the *c*. 680 Ma zircons (South Qinling) could not have been transported to the Changyang area through the EZOL, and could only have been transported along the Exi Strait (Fig. 8b′, c′). The *c*. 680 Ma age peak was found within the Exi Strait (Fig. 8a′, c′–g′), further indicating that the source material from South Qinling was transported through the Exi Strait, depositing material along the way. Nevertheless, the *c*. 680 Ma source material disappeared on the northern edge of the Jiangnan Orogenic Belt in the Guibei section (Fig. 8h′), suggesting that the JNO blocked the migration of the source material.

In summary, the transportation of material from the northern margin of the YGD to the southeast margin of the YGD occurred as early as *c*. 680 Ma, and the source material migrated mainly through the Exi Strait.

5.c. Reconstruction of the palaeogeography

As mentioned above, the magmatic rocks in the SQB were emplaced during *c*. 941 Ma to 667 Ma. The magmatic rocks recorded four major Neoproterozoic magmatic events: (1) *c*. 940 Ma, the formation of arc-related high-Nb titanite-bearing diorites; (2) *c*. 885 Ma, the formation of gabbroic to dioritic arc-related rocks; (3) 785–740 Ma, widespread magmatism with the emplacement of intermediate to felsic granitoids, showing typical arc-related characteristics; and (4) *c*. 667 Ma gabbroic magmatism, formed in an extensional setting (Hu, F. Y. *et al*. 2016). Four Neoproterozoic magmatic stages were recognized in the uplift zone of the SQB, corresponding to four magmatic stages in the northern margin of the YGD (Hu, F. Y. *et al*. 2016 and references therein). The analogous crystallization ages and petrogenesis between the Neoproterozoic blocks in the western and middle SQB and the volcanic rocks of the Wudangshan and Yaolinghe groups (Ling *et al*. 2008; Wang, L. J. *et al*. 2013; Zhu *et al*. 2014) and the Tiewadian pluton (Yang *et al*. 2012), point to a genetic correlation of the Neoproterozoic rocks in the SQB. Based on the evidence presented above, a large Neoproterozoic continental block was established in the SQB. In summary, we propose that there is a Neoproterozoic uplift zone in the SQB and the Neoproterozoic uplift was part of the northern margin of the YGD during the Neoproterozoic era. This study suggests that the uplift was a source of the study area strata (Fig. 9).

During early Neoproterozoic time (1.0–0.9 Ga), the ancient South China oceanic plate subducted beneath the southern margin of the YGD, forming an active continental margin. Subsequently, the ocean was closed, forming the Jiangshan– Shaoxing–Pingxiang ophiolitic melange belt. At 850–820 Ma, the Yangtze and Cathaysia domains completed collision and formed the Jiangnan Orogenic Belt (Shu, 2012). The southeast margin of the Jiangnan Orogenic

https://doi.org/10.1017/S0016756818000535 Published online by Cambridge University Press

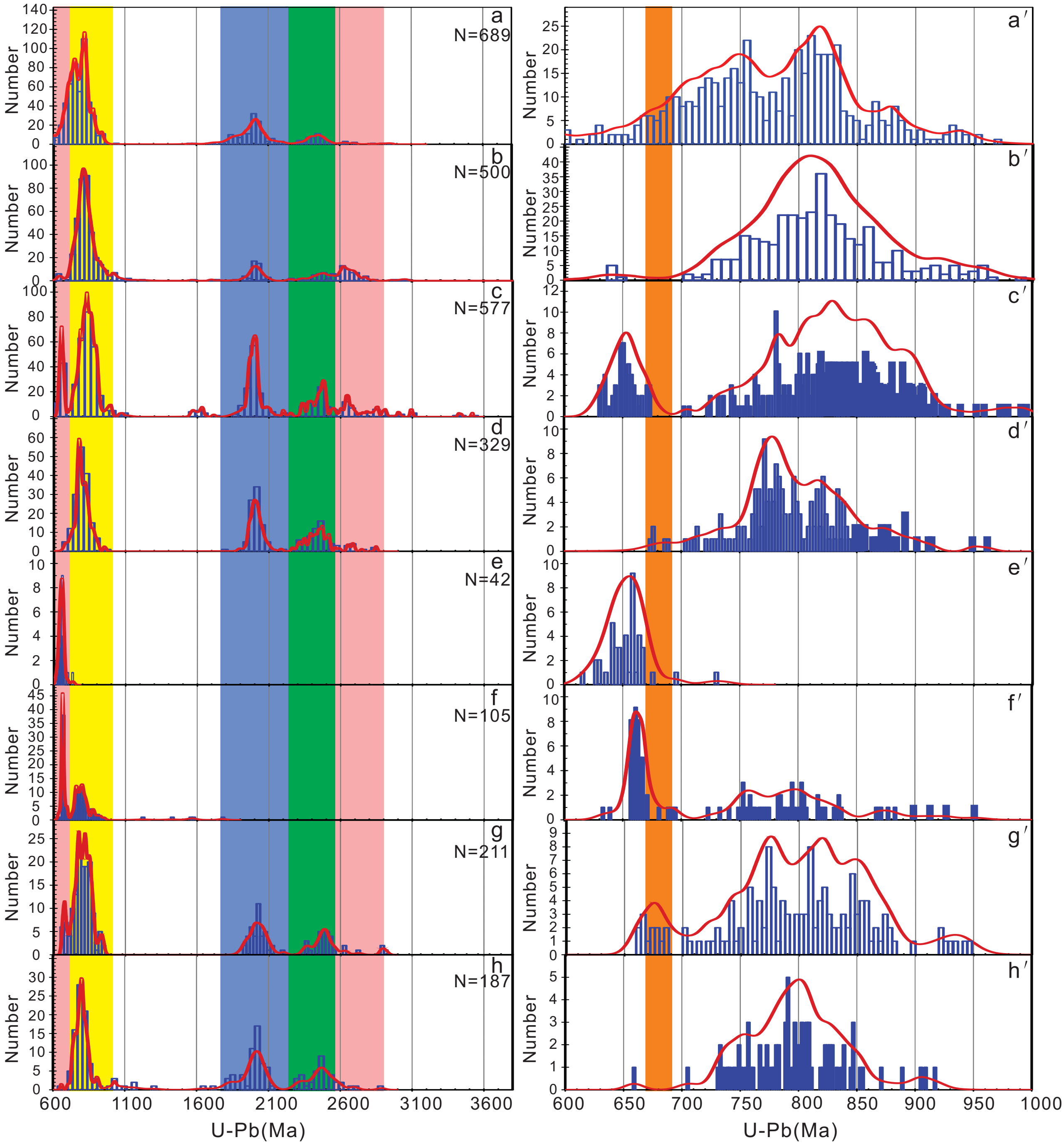

Figure 8. (Colour online) The U–Pb age of the Nanhua System (720–635 Ma) distributed in the Yangtze Domain. (a, a′) Wudangshan section (Ling *et al*. 2010; Wang, L. J. *et al*. 2013); (b, b′) Yichang section (Hofmann *et al*. 2011; Pi & Jiang, 2016; Hu, R. *et al*. 2016); (c, c′) Changyang section (Liu, X. M. *et al*. 2008; Liu *et al*. 2015); (d, d′) Shimen section (Lan *et al*. 2015; Wang *et al*. 2012*a*); (e, e′) Guzhang section (Zhang, Jiang & Han, 2008); (f, f′) Songtao section (Yin *et al*. 2006; Wang *et al*. 2010; Yu *et al*. 2016); (g, g′) Anhua section (the data in this study); (h, h′) Guibei section (Gao *et al*. 2013; Han *et al*. 2016; and some unpub. data).

Belt developed S-type granite with an estimated age of 820 Ma (Shu, 2006 and references therein). The intense collisional orogeny resulted in the formation of large areas of shallow metamorphic rocks. All of these suggest that the ancient South China plate formed after the long tectonic evolution of the Precambrian.

After 820 Ma, the South China Block entered the intraplate-rifting stage, corresponding to cracking of the Rodinia supercontinent, forming the Nanhua rift and Chuandian rift basins. Corresponding rift-type magmatic activities gave rise to formations, such as the bimodal volcanic rocks (Tiechuanshan Formation (817 ± 5 Ma), Suxiong Formation (803 ± 12 Ma) and the Taoyuan Formation (818 ± 12 Ma)) (Wang & Li, 2003). It also included the earlier basal magmatic activity (840–790 Ma) along the Zhenghe–Dapu fault (Shu, 2012). The South China Block, which was composed of the Yangtze and the Cathaysia domains, cracked and formed the different terranes and rift basins (Fig. 2).

https://doi.org/10.1017/S0016756818000535 Published online by Cambridge University Press

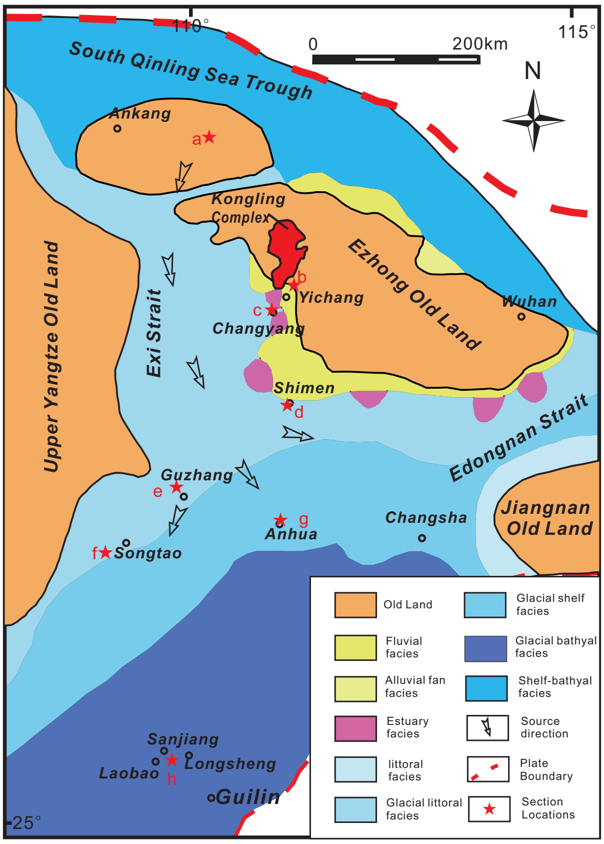

Figure 9. (Colour online) Source migration palaeogeographic map of South China during deposition of the middle–upper Nanhua System. (a – Wudang section; b – Yichang section; c – Changyang section; d – Shimen section; e – Guzhang section; f – Songtao section; g – Anhua section; h – Guibei section.)

6. Conclusions

(1) The U–Pb ages of the youngest detrital zircon grains from the Niuguping, Gucheng and Datangpo formations yielded average ages of 712 ± 24 Ma, 679.2 ± 6.2 Ma and 665.1 ± 7.4 Ma, respectively, which correspond closely to the depositional ages of each formation.

(2) Samples from western Hunan in the middle–upper Nanhua System have six main peak ages: *c*. 680 Ma, *c*. 780 Ma, *c*.820 Ma, *c*. 940 Ma, *c*. 2000 Ma and *c*. 2500 Ma. In addition, some magmatic zircons of *c*. 2900 Ma were also identified. The characteristics of the U–Pb ages and Hf isotopes indicate that there was a link between the north and southeast margins of the YGD as early as *c*. 680 Ma, and the provenance of the coeval sedimentary sequences of the southeast YGD was South Qinling on the northern margin of the YGD. Furthermore, the *c*. 2.0 Ga metamorphic zircons also indicate that the source of the study area is South Qinling.

(3) From the analysis of the *c*. 680 Ma provenance in the YGD, we surmise that source rock materials were transported from the north to south to the southeast edge of the YGD through the Exi Strait and disappeared on the northern edge of the Jiangnan Orogenic Belt. The Exi Strait served as the main channel for the migration of materials.

Acknowledgements. This study was supported by the National Natural Sciences Foundation of China (Grant No. 41472190 and 41172189). We sincerely thank Prof. Wei Wang for constructive suggestions that have greatly improved the manuscript. We appreciate Dr. Wenchao Yu for his comments on this paper. We also acknowledge Zhaochu Hu for his assistance in the LA-ICP-MS U–Pb zircon analysis conducted at the State Key Laboratory of Geological Processes and Mineral Resources, China University of Geosciences, Wuhan.

Supplementary material

To view supplementary material for this article, please visit https://doi.org/10.1017/S0016756818000535

References

Andersen, T. 2005. Detrital zircons as tracers of sedimentary provenance: limiting conditions from statistics and numerical simulation. *Chemical Geology* **216**, 249–70.

Andersen, T., Kristoffersen, M. & Elburg, M. A. 2016. How far can we trust provenance and crustal evolution information from detrital zircons? A South African case study. *Gondwana Research* **34**, 129–48.

Barfod, G. H., Albarède, F., Knoll, A. H., Xiao, S. H., Télouk, P., Frei, R. & Baker, J. 2002. New Lu–Hf and Pb–Pb age constraints on the earliest animal fossils. *Earth and Planetary Science Letters* **201**, 203–12.

Belousova, E. A., Kostitsyn, Y. A., Griffin, W. L., Begg, G. C., O'Reilly, S. Y. & Pearson, N. J. 2012. The growth of the continental crust: constraints from zircon Hf-isotope data. *Lithos* **119**, 457–66.

Blichert-Toft, J., Chauvel, C. & Albarède, F. 1997. Separation of Hf and Lu for high-precision isotope analysis of rock samples by magnetic sector-multiple collector ICP-MS. *Contributions to Mineralogy and Petrology* **127** (3), 248–60.

Cai, Z. Y., Xiong, X. L., Luo, H., Wu, D. K., Sun, S. C., Rao, B. L. & Wang, S. Q. 2007. Forming age of the volcanic rocks of the Yaolinghe Group from Wudang block, Southern Qinling Mountain: constraint from grain-zircon U–Pb dating. *Acta Geologica Sinica* **81** (5), 620–5 (in Chinese with English abstract).

Charvet, J. 2013. The Neoproterozoic–Early Paleozoic tectonic evolution of the South China Block: an overview. *Journal of Asian Earth Sciences* **74**, 198–209.

Chen, Q., Sun, M., Long, X., Zhao, G. C., Wang, J., Yu, Y. & Yuan, C. 2016. U–Pb ages and Hf isotopic record of zircons from the late Neoproterozoic and Silurian–Devonian sedimentary rocks of the western Yangtze Block: implications for its tectonic evolution and continental affinity. *Gondwana Research* **31**, 184–99.

Chen, Q., Sun, M., Long, X., Zhao, G. C., Wang, J., Yu, Y. & Yuan, C. 2018. Provenance study for the Paleozoic sedimentary rocks from the West Yangtze Block: constraint on possible link of South China to the Gondwana supercontinent reconstruction. *Precambrian Research* **309**, 271–89.

Chen, D. F., Dong, W. Q., Zhu, B. Q. & Chen, X. P. 2004. Pb–Pb ages of Neoproterozoic Doushantuo phosphorites in South China: constraints on early metazoan evolution and glaciation events. *Precambrian Research* **132**, 123–32.

CHINESE ACADEMY OF GEOLOGICAL SCIENCES (CAGS). 2004. *Geological Map of China, Scale 1:2,500,000*. Beijing: Geological Publishing House (in Chinese).

CHU, X. L., TODT, W., ZHANG, Q. R., CHEN, F. K. & HUANG, J. 2005. U–Pb zircon age for the Nanhua–Sinian boundary. *Chinese Science Bulletin* **50**, 716–8.

CONDON, D., ZHU, M. Y., BOWRING, S., WANG, W., YANG, A. H. & JIN, Y. G. 2005. U–Pb ages from the Neoproterozoic Doushantuo Formation. *China: Science* **308**, 95–8.

DONG, Y. P. & SANTOSH, M. 2016. Tectonic architecture and multiple orogeny of the Qinling Orogenic Belt, Central China. *Gondwana Research* **29**, 1–40.

DONG, Y. P., ZHANG, G. W., NEUBAUER, F., LIU, X. M., GENSER, J. & HAUZENBERGER, C. 2011. Tectonic evolution of the Qinling orogen, China: review and synthesis. *Journal of Asian Earth Sciences* **41**, 213–37.

DU, Q. D., WANG, Z. J., WANG, J., QIU, Y. S., JIANG, X. S., DENG, Q. & YANG, F. 2013. Geochronology and paleoenvironment of the pre-Sturtian glacial strata: evidence from the Liantuo Formation in the Nanhua rift basin of the Yangtze Block, South China. *Precambrian Research* **233**, 118–31.

FANNING, C. M. & LINK, P. K. 2004. U–Pb SHRIMP ages of Neoproterozoic (Sturtian) glaciogenic Pocatello Formation, southeastern Idaho. *Geology* **32**, 881–4.

FEDO, C. M., SIRCOMBE, K. N. & RAINBIRD, R. H. 2003. Detrital zircon analysis of the sedimentary record. *Reviews in Mineralogy and Geochemistry* **53**, 277–303.

FONNELAND, H. C., LIEN, T., MARTINSEN, O. J., PEDERSEN, R. B. & KOSLER, J. 2004. Detrital zircon ages: a key to understanding the deposition of deep marine sandstones in the Norwegian Sea. *Sedimentary Geology* **164**, 147–59.

GAO, L. Z., LU, J. P., DING, X. Z., WANG, H. R., LIU, X. Y. & LI, J. 2013. Zircon U–Pb dating of Neoproterozoic tuff in South Guangxi and its implications for stratigraphic correlation. *Geology in China*. **40** (5), 1443–52.

GEHRELS, G. E. 2012. Detrital zircon U–Pb geochronology: current methods and new opportunities. In *Tectonics of Sedimentary Basins: Recent Advances* (eds C. Busby & A. Azor), pp. 45–62. Oxford, UK: Blackwell Publishing Ltd.

GUO, X. Q., YAN, Z., WANG, Z. Q., FU, C. L. & CHEN, L. 2014. Tectonic setting of Lijiabian Ti–Fe deposit in Shanyang–Zhashui ore concentration area, Qinling Orogen. *Acta Petrologica Sinica* **30** (2), 437–50.

HAN, K. Y., WANG, L, DING, X. Z., REN, L. D., GAO, L. Z., LIU, Y. X., PANG, J. F. & XUE, J. H. 2016. Provenance of sedimentary rocks of Nanhua System in the northern Guangxi Province: evidence from detrital zircon U–Pb ages. *Acta Petrologica Sinica* **32** (7), 2166–80 (in Chinese with English abstract).

HOFMANN, H., LINNEMANN, U., RAI, V., BAECKER, S., GÄRTNER, A. & SAGAWE, A. 2011. The India and South China cratons at the margin of Rodinia – synchronous Neoproterozoic magmatism revealed by LA-ICP-MS zircon analyses. *Lithos* **123**, 176–87.

HU, R., LI, S. Q., WANG, W. & CHEN, F. K. 2016. Source characteristics of tillite in the Nantuo Formation in the Three Gorges, Northern Yangtze Block: evidences from zircon ages and geochemical composition. *Earth Science* **41** (10), 1630–54 (in Chinese with English abstract).

HU, J., LIU, X. C., CHEN, L. Y., QU, W., LI, H. K. & GENG, J. Z. 2013. A ~2.5 Ga magmatic event at the northern margin of the Yangtze craton: evidence from U–Pb dating and Hf isotope analysis of zircons from the Douling Complex in the South Qinling Orogen. *Chinese Science Bulletin* **58** (28–29), 3564–79.

HU, Z. C., LIU, Y. S., GAO, S., LIU, W. G., YANG, L., ZHANG, W., TONG, X. R., LIN, L., ZONG, K. Q., LI, M., CHEN, H. H. & ZHOU, L. 2012a. Improved in situ Hf isotope ratio analysis of zircon using newly designed X skimmer cone and Jet sample cone in combination with the addition of nitrogen by laser ablation multiple collector ICP-MS. *Journal of Analytical Atomic Spectrometry* **27**, 1391–9.

HU, Z. C., LIU, Y. S., GAO, S., XIAO, S. Q., ZHAO, L. S., GÜNTHER, D., LI, M., ZHANG, W. & ZONG, K. Q. 2012b. A "wire" signal smoothing device for laser ablation inductively coupled plasma mass spectrometry analysis. *Spectrochimica Acta Part B: Atomic Spectroscopy* **78**, 50–7.

HU, F. Y., LIU, S. W., SANTOSH, M., DENG, Z. B., WANG, W., ZHANG, W. Y. & YAN, M. 2016. Chronology and tectonic implications of Neoproterozoic blocks in the South Qinling Orogenic Belt, Central China. *Gondwana Research* **30**, 24–47.

JAHN, B. M., GALLET, S. & HAN, J. M. 2001. Geochemistry of the Xining, Xifeng, and Jixian sections, Loess Plateau of China: eolian dust provenance and paleosol evolution during the last 140 ka. *Chemical Geology* **178**, 71–94.

LAN, Z. W., LI, X. H., ZHU, M. Y., ZHANG, R. R. & LI, Q. R. 2015. Revisiting the Liantuo Formation in Yangtze Block, South China: SIMS U–Pb zircon age constraints and regional and global significance. *Precambrian Research* **263**, 123–41.

LI, Z. X., BOGDANOVA, S. V., COLLINS, A. S., DAVIDSON, A., DE WAELE, B., ERNST, R. E., FITZSIMONS, I. C. W., FUNK, R. A., GLADKOCHUB, D. P., JACOBS, J., KARLSTROM, K. E., LU, S., NATAPOV, L. M., PEASE, V., PISAREVSKY, S. A., THRANE, K. & VERNIKOVSKY, V. 2008. Assembly, configuration, and break-up history of Rodinia: a synthesis. *Precambrian Research* **160**, 179–210.

LI, X. H., LI, W. X. & HE, B. 2012. Building of the South China Block and its relevance to assembly and breakup of Rodinia Supercontinent: observations, interpretations and tests. *Bulletin of Mineralogy, Petrology and Geochemistry* **31** (6), 543–59 (in Chinese with English abstract).

LI, J. H., ZHANG, Y. Q., XU, X. B., DONG, S. W. & LI, T. D. 2012. Zircon U–Pb LA-ICP-MS dating of Fenghuangshan pluton in Northern Daba mountains and its implications to tectonic settings. *Geological Review* **58**, 581–93 (in Chinese with English abstract).

LING, W. L., DUAN, R. C., LIU, X. M., CHENG, J. P., MAO, X. W., PENG, L. H., LIU, Z. X., YANG, H. M. & REN, B. F. 2010. U–Pb dating of detrital zircons from the Wudangshan Group in the South Qinling and its geological significance. *Chinese Science Bulletin* **55** (22), 2440–8.

LING, W. L., REN, B. F., DUAN, R. C., LIU, X. M., MAO, X. W., PENG, L. H., LIU, Z. X., CHENG, J. P. & YANG, H. M. 2008. Timing of the Wudangshan, Yaolinghe volcanic sequences and mafic sills in South Qinling: U–Pb zircon geochronology and tectonic implication. *Chinese Science Bulletin* **53** (14), 2192–9.

LINOL, B., DE WIT, M. J., BARTON, E., DE WIT, M. J. C. & GUILLOCHEAU, F. 2016. U–Pb detrital zircon dates and source provenance analysis of Phanerozoic sequences in the Congo Basin, central Gondwana. *Gondwana Research* **29**, 208–19.

LIU, X. M., GAO, S., DIWU, C. R. & LING, W. L. 2008. Precambrian crustal growth of Yangtze craton as revealed by detrital zircon studies. *American Journal of Science* **308**, 421–68.

LIU, Y. S., GAO, S., HU, Z. C., GAO, C. G., ZONG, K. Q. & WANG, D. B. 2010a. Continental and oceanic crust recycling-induced melt-peridotite interactions in the Trans-North China Orogen: U–Pb dating, Hf isotopes and trace elements in zircons of mantle xenoliths. *Journal of Petrology* **51**, 537–71.

LIU, Y. S., HU, Z. C., GAO, S., GÜNTHER, D., XU, J., GAO, C. G. & CHEN, H. H. 2008. In situ analysis of major and trace elements of anhydrous minerals by LA-ICP-MS without applying an internal standard. *Chemical Geology* **257** (1-2), 34–43.

LIU, Y. S., HU, Z. C., ZONG, K. Q., GAO, C. G., GAO, S., XU, J. & CHEN, H. H. 2010b. Reappraisement and refinement of zircon U–Pb isotope and trace element analyses by LA-ICP-MS. *Chinese Science Bulletin* **55** (15), 1535–46.

LIU, P. J., LI, X. H., CHEN, S. M., LAN, Z. W., YANG, B., SHANG, X. D. & YIN, C. Y. 2015. New SIMS U–Pb zircon age and its constraint on the beginning of the Nantuo glaciation. *Science Bulletin* **60**, 958–63.

LIU, R. Y., NIU, B. G., HE, Z. J. & REN, J. S. 2011. LA-ICP-MS zircon U–Pb geochronology of the eastern part of the Xiaomaoling composite intrusives in Zhashui area, Shansnxi, China. *Geological Bulletin of China* **30** (2/3), 448–60 (in Chinese with English abstract).

LIU, C. H., WU, C. L., GAO, Y. H., LEI, M., QIN, H. P. & LI, M. Z. 2014. Zircon LA-ICP-MS U–Pb dating and Lu–Hf isotopic system of Dongjiangkou, Zhashui, and Liyuantang granitoid intrusions, South Qinling belt, central China. *Acta Petrologica Sinica* **30** (8), 2402–20 (in Chinese with English abstract).

LIU, B. J. & XU, X. S. 1994. *The Paleogeographic Atlas in South China*. Beijing: Science Press, 1–188 pp. (in Chinese).

LUDWIG, K. R. 2003. *ISOPLOT 3.00: A Geochronological Toolkit for Microsoft Excel*. California, Berkeley: Berkeley Geochronology Center, 39 pp.

MCCULLOCH, M. T., ROSMAN, K. J. R. & DE LAETER, J. R. 1977. The isotopic and elemental abundance of ytterbium in meteorites and terrestrial samples. *Geochimica et Cosmochimica Acta* **41**, 1703–7.

MCLENNAN, S. M. 2001. Relationships between the trace element composition of sedimentary rocks and upper continental crust. *Geochemistry, Geophysics, Geosystems* **2**, doi: 10.1029/2000GC000109.

MYROW, P. M., HUGHES, N. C., GOODGE, J. W., FANNING, C. M., WILLIAMS, I. S., PENG, S. C., BHARGAVA, O. N., PARCHA, S. K. & POGUE, K. R. 2010. Extraordinary transport and mixing of sediment across Himalayan central Gondwana during the Cambrian–Ordovician. *Geological Society of America Bulletin* **122**, 1660–70.

NIE, H., YAO, J., WAN, X., ZHU, X. Y., WOLFGANG, S. & CHEN, F. K. 2016. Precambrian tectonothermal evolution of South Qinling and its affinity to the Yangtze Block: evidence from zircon ages and Hf–Nd isotopic compositions of basement rocks. *Precambrian Research* **286**, 167–79.

NIU, B. G., HE, Z. J., REN, J. S., WANG, J. & DENG, P. 2006. SHRIMP U–Pb ages of zircons from the intrusions in the western Douling–Xiaomaoling Uplift and their geological significances. *Geological Review* **52**, 826–35 (in Chinese with English abstract).

PI, D. H. & JIANG, S. Y. 2016. U–Pb dating of zircons from tuff layer, sandstone and tillite samples in the uppermost Liantuo Formation and the lowermost Nantuo Formation in Three Gorges area, South China. *Chemie der Erde* **76**, 103–9.

QIU, Y. M., GAO, S., MCNAUGHTON, N. J., GROVES, D. I. & LING, W. L. 2000. First evidence of ≥3.2 Ga continental crust in the Yangtze craton of South China and its implications for Archean crustal evolution and Phanerozoic tectonics. *Geology* **28**, 11–4.

RAINBIRD, R. H., HAMILTON, M. A. & YOUNG, G. M. 2001. Detrital zircon geochronology and provenance of the Torridonian, NW Scotland. *Journal of the Geological Society, London* **158**, 15–27.

RUDNICK, R. L. & GAO, S. 2003. Composition of the continental crust. In *Treatise on Geochemistry, Volume 3* (ed. R. L. Rudnick), pp. 1–64.

SHI, Y., YU, J. H. & SANTOSH, M. 2013. Tectonic evolution of the Qinling orogenic belt, Central China: new evidence from geochemical, zircon U–Pb geochronology and Hf isotopes. *Precambrian Research* **231**, 19–60.

SHU, L. S. 2006. Predevonian tectonic evolution of South China: from Cathaysian Block to Caledonian period folded orogenic belt. *Geological Journal of China Universities* **12** (4), 418–31.

SHU, L. S. 2012. An analysis of principal features of tectonic evolution in South China Block. *Geological Bulletin of China* **31** (7), 1035–53.

SUN, M., CHEN, N. S., ZHAO, G. C., WILDE, S. A., YE, K., GUO, J. H., CHEN, Y. & YUAN, C. 2008. U–Pb zircon and Sm–Nd isotopic study of the Huangtuling granulite, Dabie–Sulu belt, China: implication for the Paleoproterozoic tectonic history of the Yangtze craton. *American Journal of Science* **308**, 469–83.

WANG, W., CAWOOD, P. A., ZHOU, M. F., PANDIT, M. K. & CHEN, W. T. 2017. Zircon U–Pb age and Hf isotope evidence for an Eoarchean crustal remnant and episodic crustal reworking in response to supercontinent cycles in NW India. *Journal of the Geological Society, London* **174**, 759–72.

WANG, W., CAWOOD, P. A., ZHOU, M. F. & ZHAO, J. H., 2016. Paleoproterozoic magmatic and metamorphic events link Yangtze to northwest Laurentia in the Nuna supercontinent. *Earth and Planetary Science Letters* **433**, 269–79.

WANG, W., CHEN, F. K., HU, R., CHU, Y. & YANG, Y. Z. 2012a. Provenance and tectonic setting of Neoproterozoic sedimentary sequences in the South China Block: evidence from detrital zircon ages and Hf–Nd isotopes. *International Journal of Earth Sciences (Geologische Rundschau)* **101**, 1723–44.

WANG, L. J., GRIFFIN, W. L., YU, J. H. & O'REILLY, S. Y. 2010. Precambrian crustal evolution of the Yangtze Block tracked by detrital zircons from Neoproterozoic sedimentary rocks. *Precambrian Research* **177** (1), 131–44.

WANG, L. J., GRIFFIN, W. L., YU, J. H. & O'REILLY, S. Y. 2013. U–Pb and Lu–Hf isotopes in detrital zircon from Neoproterozoic sedimentary rocks in the northern Yangtze Block: implications for Precambrian crustal evolution. *Gondwana Research* **23**, 1261–72.

WANG, J. & LI, Z. X. 2003. History of Neoproterozoic rift basins in South China: implications for Rodinia break-up. *Precambrian Research* **122**, 141–58.

WANG, R. R., XU, Z. Q., SANTOSH, M., YAO, Y., GAO, L. E. & LIU, C. H. 2016. Late Neoproterozoic magmatism in South Qinling, Central China: geochemistry, zircon U–Pb–Lu–Hf isotopes and tectonic implications. *Tectonophysics* **683**, 43–61.

Wang, X. L., Zhou, J. C., Qiu, J. S., Liu, X. M. & Zhang, G. L. 2006. LA-ICP-MS U–Pb zircon geochronology of the Neoproterozoic igneous rocks from Northern Guangxi, South China: implications for tectonic evolution. *Precambrian Research* **145**, 111–30.

Wang, W., Zhou, M. F., Yan, D. P. & Li, J. W. 2012b. Depositional age, provenance, and tectonic setting of the Neoproterozoic Sibao Group, southeastern Yangtze Block, South China. *Precambrian Research* **192–195**, 107–24.

Wang, W., Zhou, M. F., Yan, D. P., Li, L. & John, M. 2013. Detrital zircon record of Neoproterozoic active-margin sedimentation in the eastern Jiangnan Orogen, South China. *Precambrian Research* **235**, 1–19.

Woodhead, J., Hergt, J., Shelley, M., Eggins, S. & Kemp, R. 2004. Zircon Hf-isotope analysis with an excimer laser, depth profiling, ablation of complex geometries, and concomitant age estimation. *Chemical Geology* **209**, 121–35.

Wu, Y. B., Chen, D. G., Xia, Q. K., Deloule, E. & Chen, H. 2002. SIMS U–Pb dating of zircons in granulite of Huangtuling from Northern Dabieshan. *Acta Petrologica Sinica* **18** (3), 378–82 (in Chinese with English abstract).

Wu, Y. B., Gao, S., Gong, H. J., Xiang, H., Jiao, W. F., Yang, S. H., Liu, Y. S. & Yuan, H. L. 2009. Zircon U–Pb age, trace element and Hf isotope composition of Kongling terrane in the Yangtze Craton: refining the timing of Palaeoproterozoic high-grade metamorphism. *Journal of Metamorphic Geology* **27** (6), 461–77.

Wu, Y. B., Gao, S., Zhang, H., Zheng, J. P., Liu, X., Wang, H., Gong, H., Zhou, L. & Yuan, H. 2012. Geochemistry and zircon U–Pb geochronology of Paleoproterozoic arc related granitoid in the northwestern Yangtze Block and its geological implications. *Precambrian Research* **200**, 26–37.

Wu, F. F., Wang, Z. Q., Wang, T., Yan, Z. & Chen, L. 2012. SHRIMP zircon U–Pb ages and geochemical characteristics of the Banbanshan K-feldspar granite in Shanyang, Southern Qinling Orogenic Belt. *Journal of Mineralogy and Petrology* **32** (2), 63–73 (in Chinese with English abstract).

Wu, Y. B., Zhou, G. Y., Gao, S., Liu, X. C., Qin, Z. W., Wang, H., Yang, J. Z. & Yang, S. H. 2014. Petrogenesis of Neoarchean TTG rocks in the Yangtze Craton and its implication for the formation of Archean TTGs. *Precambrian Research* **254**, 73–86.

Xia, L. Q., Xia, Z. C., Li, X. M., Ma, Z. P. & Xu, X. Y. 2008. Petrogenesis of the Yaolinghe Group, Yunxi Group, Wudangshan Group volcanic rocks and basic dyke swarms from eastern part of the South Qinling mountains. *Northwestern Geology* **41** (3), 1–29 (in Chinese with English abstract).

Xia, Y., Xu, X., Niu, Y. & Liu, L. 2018. Neoproterozoic amalgamation between Yangtze and Cathaysia blocks: the magmatism in various tectonic settings and continent-arc-continent collision. *Precambrian Research* **309**, 56–87.

Xiao, S. H., Tucker, R., Peng, Z. X. & Zhou, C. M. 2004. New constraints on the ages of Neoproterozoic glaciations in South China. *Geology* **32**, 437–40.

Yan, M., Liu, S. W., Li, Q. G., Yang, P. T., Wang, W., Guo, R. R., Bai, X. & Deng, Z. B. 2014. LA-ICP-MS zircon U–Pb chronology and Lu–Hf isotopic features of the Mihunzhen pluton in the South Qinling tectonic belt. *Acta Petrologica Sinica* **30** (2), 390–400.

Yang, P. T., Liu, S. W., Li, Q. G., Wang, Z. Q., Wang, W. & Bai, X. 2012. Emplacing age of the Tiewadian pluton in the South Qinling tectonic belt and its geological implications. *Acta Geologica Sinica* **86**, 1525–40 (in Chinese with English abstract).

Yang, Z. N., Yang, K. G., Polat, A. & Xu, Y. 2018. Early crustal evolution of the eastern Yangtze Block: evidence from detrital zircon U–Pb ages and Hf isotopic composition of the Neoproterozoic Huashan Group in the Dahongshan Area. *Precambrian Research* **309**, 248–70.

Yin, C. Q., Lin, S. F., Davis, D. W., Zhao, G. C., Xiao, W. J., Li, L. M. & He, Y. H., 2013. 2.1–1.85 Ga tectonic events in the Yangtze Block, South China: petrological and geochronological evidence from the Kongling Complex and implications for the reconstruction of supercontinent Columbia. *Lithos* **182**, 200–10.

Yin, C. Y, Tang, F., Liu, Y. Q., Gao, L. Z., Liu, P. J., Xing, Y. S., Yang, Z. Q., Wan, Y. S. & Wang, Z. Q. 2005a. U–Pb zircon age from the base of the Ediacaran Doushantuo Formation in the Yangtze Gorges, South China: constraint on the age of Marinoan glaciation. *Episodes* **28**, 48–9.

Yin, C. Y., Tang, F., Liu, Y. Q., Gao, L. Z., Yang, Z. Q., Wang, Z. Q., Liu, P. J., Xing, Y. S. & Song, B. 2005b. New U–Pb zircon ages from the Ediacaran (Sinian) System in the Yangtze Gorges: constraint on the age of Miaohe biota and Marinoan glaciation. *Geological Bulletin of China* **24**, 393–400.

Yin, C. Y., Wang, Y. G., Tang, F., Wan, Y. S., Wang, Z. Q., Gao, L. Z., Xing, Y. S. & Liu, P. J. 2006. SHRIMP II U–Pb zircon date from the Nanhuan Datangpo Formation in Songtao County, Guizhou Province. *Acta Geologica Sinica* **80** (2), 273–8 (in Chinese with English abstract).

Yu, W. C., Du, Y. S., Zhou, Q., Wang, P., Yuan, L. J., Xu, Y., Pan, W., Xie, X. F., Qi, L. & Jiao, L. X. 2016. LA-ICP-MS zircon U–Pb dating from the Nanhuan Datangpo Formation in Songtao Area, East Guizhou and its geological significance. *Geological Review* **3**, 539–49 (in Chinese with English abstract).

Zhang, S. H., Jiang, G. Q. & Han, Y. G. 2008. The age of the Nantuo Formation and Nantuo glaciation in South China. *Terra Nova* **20**, 289–94.

Zhang, S. H., Jiang, G. Q., Zhang, J. M., Song, B., Kennedy, M. J. & Christie-Blick, N. 2005. U–Pb sensitive high-resolution ion microprobe ages from the Doushantuo Formation in South China: constraints on late Neoproterozoic glaciations. *Geology* **33**, 473–6.

Zhang, C. L., Li, M., Wang, T., Yuan, H. L. & Yan, Y. X. 2004. U–Pb zircon geochronology and geochemistry of granitoids in the Douling Group in the Eastern Qinling. *Acta Geologica Sinica* **78** (1), 83–95.

Zhang, C. L., Santosh, M., Zhu, Q. B., Chen, X. Y. & Huang, W. C. 2015. The Gondwana connection of South China: evidence from monazite and zircon geochronology in the Cathaysia block. *Gondwana Research* **28**, 1137–51.

Zhang, J. Y., Yin, A., Liu, W. C., Wu, F. Y., Lin, D. & Grove, M. 2012. Coupled U–Pb dating and Hf isotopic analysis of detrital zircon of modern river sand from the Yalu River (Yarlung Tsangpo) drainage system in southern Tibet: constraints on the transport processes and evolution of Himalayan rivers. *Geological Society of America Bulletin* **124**, 1449–73.

Zhang, Y. Q., Zhang, J., Li, H. K. & Lu, S. N. 2013. Zircon U–Pb geochronology of the meta-acidic volcanic rocks from the Wudangshan Group, Southern Qinling Mountains, Central China. *Acta Geologica Sinica* **87** (7), 922–30 (in Chinese with English abstract).

Zhang, G. W., Zhang, B. R., Yuan, X. C. & Xiao, Q. H. 2001. *Qinling Orogenic Belt and Continental Dynamics*. Beijing: Science Press, 855 pp.

Zhang, S. B. & Zheng, Y. F. 2013. Formation and evolution of Precambrian continental lithosphere in South China. *Gondwana Research* **23**, 1241–60.

Zhang, S. B., Zheng, Y. F., Wu, Y. B., Zhao, Z. F., Gao, S. & Wu, F. Y. 2006a. Zircon U–Pb age and Hf isotope evidence for 3.8 Ga crustal remnant and episodic reworking of Archean crust in South China. *Earth and Planetary Science Letters* **252**, 56–71.

Zhang, S. B., Zheng, Y. F., Wu, Y. B., Zhao, Z. F., Gao, S. & Wu, F. Y. 2006b. Zircon isotope evidence for ≥3.5 Ga continental crust in the Yangtze craton of China. *Precambrian Research* **146**, 16–34.

Zhang, S. B., Zheng, Y. F., Wu, Y. B., Zhao, Z. F., Gao, S. & Wu, F. Y. 2006c. Zircon U–Pb age and Hf–O isotope evidence for Paleoproterozoic metamorphic event in South China. *Precambrian Research* **151**, 265–88.

Zhao, J. H., Zhou, M. F., Yan, D. P., Zheng, J. P. & Li, J. W. 2011. Reappraisal of the ages of Neoproterozoic strata in South China: no connection with the Grenvillian Orogeny. *Geology* **39**, 299–302.

Zheng, Y. F. & Zhang, S. B. 2007. Formation and evolution of Precambrian continental crust in South China. *Chinese Science Bulletin* **52** (1), 1–10 (in Chinese with English abstract).

Zhu, X. Y., Chen, F. K., Liu, B. X. & Zhang, H. 2015. Geochemistry and zircon ages of mafic dikes in the South Qinling, central China: evidence from late Neoproterozoic continental rifting in the northern Yangtze Block. *International Journal of Earth Sciences (Geologische Rundschau)* **104**, 27–44.

Zhu, X. Y., Chen, F. K., Nie, H., Siebel, W., Yang, Y. Z., Xue, Y. Y. & Zhai, M. G. 2014. Neoproterozoic tectonic evolution of South Qinling, China: evidence from zircon ages and geochemistry of the Yaolinghe volcanic rocks. *Precambrian Research* **245**, 115–30.